

SUPERNOVA EXPLOSIONS OF SUPER-ASYMPTOTIC GIANT BRANCH STARS: MULTICOLOR LIGHT CURVES OF ELECTRON-CAPTURE SUPERNOVAE

NOZOMU TOMINAGA^{1,2}, SERGEI I. BLINNIKOV^{3,2}, KEN'ICHI NOMOTO^{2,4}

Accepted for publication in the Astrophysical Journal Letters.

ABSTRACT

An electron-capture supernova (ECSN) is a core-collapse supernova explosion of a super-asymptotic giant branch (SAGB) star with a main-sequence mass $M_{\text{MS}} \sim 7 - 9.5 M_{\odot}$. The explosion takes place in accordance with core bounce and subsequent neutrino heating and is a unique example successfully produced by first-principle simulation. This allows us to derive a first self-consistent multicolor light curves of a core-collapse supernova. Adopting the explosion properties derived by the first-principle simulation, i.e., the low explosion energy of 1.5×10^{50} erg and the small ^{56}Ni mass of $2.5 \times 10^{-3} M_{\odot}$, we perform a multigroup radiation hydrodynamics calculation of ECSNe and present multicolor light curves of ECSNe of SAGB stars with various envelope mass and hydrogen abundance. We demonstrate that a shock breakout has peak luminosity of $L \sim 2 \times 10^{44}$ erg s⁻¹ and can evaporate circumstellar dust up to $R \sim 10^{17}$ cm for a case of carbon dust, that plateau luminosity and plateau duration of ECSNe are $L \sim 10^{42}$ erg s⁻¹ and $t \sim 60 - 100$ days, respectively, and that a plateau is followed by a tail with a luminosity drop by ~ 4 mag. The ECSN shows a bright and short plateau that is as bright as typical Type II plateau supernovae, and a faint tail that might be influenced by spin-down luminosity of a newborn pulsar. Furthermore, the theoretical models are compared with ECSN candidates: SN 1054 and SN 2008S. We find that SN 1054 shares the characteristics of the ECSNe. For SN 2008S, we find that its faint plateau requires a ECSN model with a significantly low explosion energy of $E \sim 10^{48}$ erg.

Subject headings: shock waves — radiative transfer — supernovae: general — stars: evolution — supernovae: individual (Crab Nebula, SN 2008S)

1. INTRODUCTION

A massive star with a main-sequence mass $M_{\text{MS}} \gtrsim 8 M_{\odot}$ ends up as a core-collapse supernova (CCSN). Core collapse is inaugurated by electron capture for a star with an O+Ne+Mg core ($M_{\text{MS}} \lesssim 10 M_{\odot}$) or Fe photodisintegration for a star with a Fe core ($M_{\text{MS}} \gtrsim 10 M_{\odot}$).

An explosion mechanism of CCSNe is still under investigation, in particular, for the CCSN of the star with the Fe core (Fe CCSN). Recently, sophisticated multidimensional simulation finds that neutrino-driven convection and/or standing-accretion shock instability (SASI) enhances neutrino heating and initiates an outward flow (e.g., Janka et al. 2012; Kotake et al. 2012; Burrows 2013; Bruenn et al. 2013, for recent reviews). However, explosion energies E are about one orders of magnitude smaller than a canonical value of a normal CCSN ($E \sim 10^{51}$ erg, e.g., SN 1987A Blinnikov et al. 2000).

A fate of the less-massive star with the O+Ne+Mg core is different from that of the star with the Fe core (Miyaji et al. 1980; Nomoto et al. 1982; Nomoto 1984, 1987; Miyaji & Nomoto 1987). The O+Ne+Mg core is supported by electron degenerate pressure. A mass and

density of the O+Ne+Mg core increase through phases of shell burning of He and H. As the O+Ne+Mg core grows, an envelope undergoes mass loss to reduce the H mass and He dredge-up to enhance He abundance. Eventually, the star becomes a super-asymptotic giant branch (SAGB) star (e.g., Siess 2007). When central density exceeds a critical value (4×10^{12} kg m⁻³), electrons start to be captured by magnesium, the degenerate pressure decreases, and thus the O+Ne+Mg core collapses gravitationally (Miyaji et al. 1980; Nomoto et al. 1982).

Ensuing core bounce and neutrino heating can eject the envelope and a part of the O+Ne+Mg core because of weak inward momentum carried by the low-density SAGB envelope (Kitaura et al. 2006; Burrows et al. 2007; Janka et al. 2008). The explosion is called an electron-capture supernova (ECSN, Nomoto 1984, 1987). In contrast to the Fe CCSN, the explosion of the ECSN is realized by first-principle simulation (Kitaura et al. 2006; Burrows et al. 2007; Janka et al. 2008) and 2D simulation demonstrates that the explosion takes place almost spherically (Janka et al. 2008). This is the only example of the CCSN being self-consistently produced. However, a low explosion energy derived from the simulation ($E \sim 10^{50}$ erg) discriminates the ECSN from normal CCSNe.

The first-principle hydrodynamics simulation enables self-consistent studies, e.g., on nucleosynthesis and observational features. Explosive nucleosynthesis in the ECSN is calculated by Hoffman et al. (2008) and Wanajo et al. (2009) based on Kitaura et al. (2006). They find a small amount of ^{56}Ni in the ejecta [$M(^{56}\text{Ni}) \sim 0.003 M_{\odot}$] and large production of elements

¹ Department of Physics, Faculty of Science and Engineering, Konan University, 8-9-1 Okamoto, Kobe, Hyogo 658-8501, Japan; tominaga@konan-u.ac.jp

² Kavli Institute for the Physics and Mathematics of the Universe (WPI), The University of Tokyo, 5-1-5 Kashiwanoha, Kashiwa, Chiba 277-8583, Japan

³ Institute for Theoretical and Experimental Physics (ITEP), Moscow 117218, Russia; Sergei.Blinnikov@itep.ru

⁴ Department of Astronomy, School of Science, The University of Tokyo, Bunkyo-ku, Tokyo 113-0033, Japan; nomoto@astron.s.u-tokyo.ac.jp

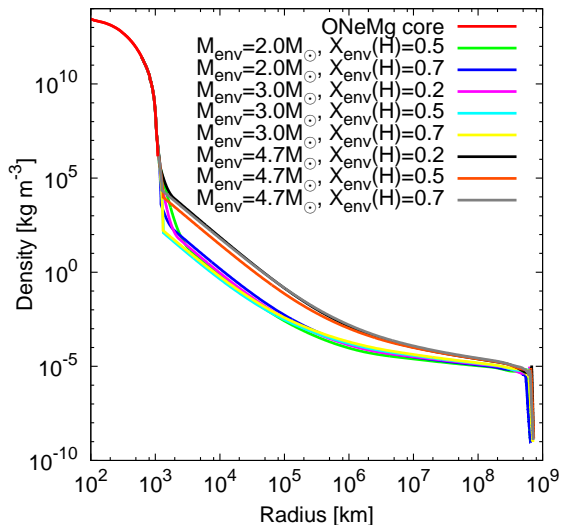


FIG. 1.— Presupernova structures of SAGB stars with $M_{\text{env}} = 2.0M_{\odot}$ and $X_{\text{env}}(\text{H}) = 0.5$ (green), $M_{\text{env}} = 2.0M_{\odot}$ and $X_{\text{env}}(\text{H}) = 0.7$ (blue), $M_{\text{env}} = 3.0M_{\odot}$ and $X_{\text{env}}(\text{H}) = 0.2$ (magenta), $M_{\text{env}} = 3.0M_{\odot}$ and $X_{\text{env}}(\text{H}) = 0.5$ (cyan), $M_{\text{env}} = 3.0M_{\odot}$ and $X_{\text{env}}(\text{H}) = 0.7$ (yellow), $M_{\text{env}} = 4.7M_{\odot}$ and $X_{\text{env}}(\text{H}) = 0.2$ (black), $M_{\text{env}} = 4.7M_{\odot}$ and $X_{\text{env}}(\text{H}) = 0.5$ (orange), and $M_{\text{env}} = 2.0M_{\odot}$ and $X_{\text{env}}(\text{H}) = 0.7$ (gray) sitting on the $1.377M_{\odot}$ O+Ne+Mg core (red).

with $Z = 30 - 40$. The small ^{56}Ni mass is also decidedly different from the normal CCSNe with $M(^{56}\text{Ni}) \sim 0.07M_{\odot}$. However, a theoretical light curve of the ECSN has not been presented and the observational features of the ECSN are not theoretically clarified yet.

There are several SNe suggested to be the ECSNe. One of old examples is Crab Nebula being a remnant of SN 1054. This is suggested from high He abundance (MacAlpine & Satterfield 2008), small ejecta mass (Fesen et al. 1997), and low kinetic energy (Frail et al. 1995). One of recent examples is SN 2008S (Prieto et al. 2008; Botticella et al. 2009), which is suggested from a dust-surrounding bright progenitor and its faintness and slow evolution. Other SN 2008S-like objects also have been discovered (e.g., Bond et al. 2009; Szczygiel et al. 2012).

In this Letter, we adopt the explosion properties derived by the state-of-art first-principle simulation and present first self-consistent multicolor light curves of ECSNe. We also investigate contribution from continuous energy release from a central remnant as the Crab pulsar. Finally, we compare the multicolor light curves with observations of ECSN candidates.

2. MODEL

We take an O+Ne+Mg core model with $1.377M_{\odot}$ at a presupernova stage from Nomoto et al. (1982) and Nomoto (1984, 1987). The model is a core of a star with $M_{\text{MS}} = 8.8M_{\odot}$ which is calculated from a He star with $2.2M_{\odot}$. A mass range of stars with the O+Ne+Mg core is $M_{\text{MS}} \sim 7 - 9.5M_{\odot}$ but a progenitor of the ECSN should possess a SAGB envelope (Langer 2012, for a review), of which mass and abundance are influenced by M_{MS} , mass loss, and third dredge-up associated with thermal pulses. However, the mass loss are highly uncertain and no calculation of full thermal pulses has been available. For almost fully convective envelope models of the progenitor, therefore, we adopt various envelope

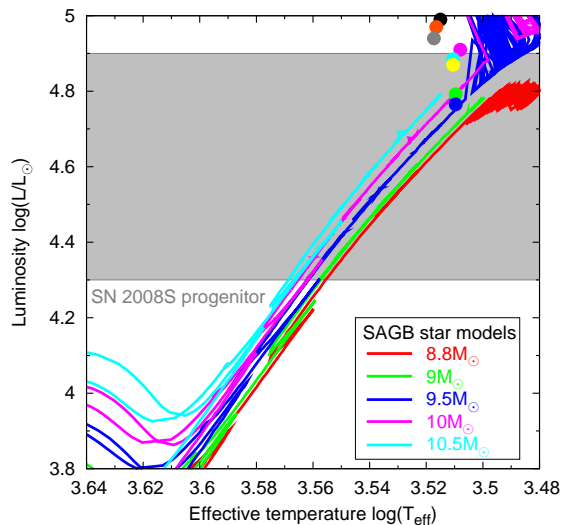


FIG. 2.— Color-magnitude diagram of SAGB stars. The adopted progenitor models (filled circles; colors are the same as Fig. 1) is compared with evolutionary models of SAGB stars with various M_{MS} [lines, $M_{\text{MS}} = 8.8M_{\odot}$ (red), $9M_{\odot}$ (green), $9.5M_{\odot}$ (blue), $10M_{\odot}$ (magenta), and $10.5M_{\odot}$ (cyan), Siess 2007] and the luminosity range of the progenitor of SN 2008S (shaded gray region, Prieto et al. 2008; Botticella et al. 2009). L_{\odot} is the solar luminosity.

mass M_{env} ($= 2.0 - 4.7M_{\odot}$) and hydrogen abundance $X_{\text{env}}(\text{H})$ ($= 0.2 - 0.7$) by constructing hydrostatic and thermal equilibrium envelopes with binding energies of $< 10^{47}$ erg (e.g., Saio et al. 1988). Density structures are shown in Figure 1. Luminosity of the progenitor models is $L \sim 3 \times 10^{38}$ erg s^{-1} (Nomoto 1987) and their radii are $R \sim 7 \times 10^8$ km. Figure 2 demonstrates that the luminosity is roughly consistent with the progenitor of SN 2008S (Prieto et al. 2008; Botticella et al. 2009) and is located at a bright tip of the SAGB stars (Siess 2007).

The explosion is initiated by a thermal bomb⁵ with the explosion energy derived by the first-principle simulation ($E = 1.5 \times 10^{50}$ erg, e.g., Kitaura et al. 2006). Subsequent evolution is followed by a multigroup radiation hydrodynamical code STELLA (Blinnikov et al. 1998, 2000, 2006), in which one-group γ -ray transfer is calculated and in situ absorption of positron is assumed for energy deposition from ^{56}Ni - ^{56}Co radioactive decay. Abundance distribution in the O+Ne+Mg core after the explosion and mass of heavy elements are taken from Model ST in Wanajo et al. (2009), which yields $2.5 \times 10^{-3}M_{\odot}$ of ^{56}Ni . We note that no ^{56}Ni is synthesized in the envelope due to low temperature of $< 2 \times 10^9$ K.

We also investigate contribution from pulsar spin-down luminosity that could be bright at birth. For example, initial spin-down luminosity of the Crab pulsar was 3.3×10^{39} erg s^{-1} .⁶ Since the pulsar spin-down luminosity can vary on individual ECSNe and deposition efficiency of an energy released from the pulsar is unknown, we expediently adopt the initial spin-down luminosity of the

⁵ This does not affect the result because a thermal energy is efficiently converted to a kinetic energy by the steep density gradient until a shock emerges from a stellar surface (§ 3).

⁶ This is estimated from current spin-down luminosity ($L_{\text{sd}} \sim 5 \times 10^{38}$ erg s^{-1} , Hester 2008) with an equation $L_{\text{sd}}(t) = L_{\text{sd},0}/(1+t/\tau_{\text{sd}})^{(n+1)/(n-1)}$, where $L_{\text{sd},0}$, τ_{sd} ($= 700$ yr) and n ($= 2.5$) are initial spin-down luminosity, a spin-down timescale, and a braking index of the Crab pulsar, respectively.

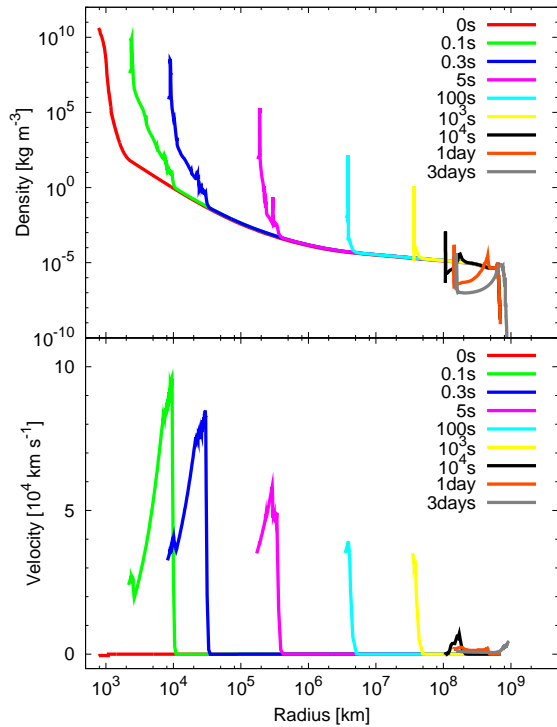


FIG. 3.— Density (a) and velocity (b) structures of the ECSN of the SAGB star with $M_{\text{env}} = 3.0M_{\odot}$ and $X_{\text{env}}(\text{H}) = 0.2$ at 0 s (red), 0.1 s (green), 0.3 s (blue), 5 s (magenta), 100 s (cyan), 10^3 s (yellow), 10^4 s (black), 1 day (orange), and 3 days (gray) after the core collapse.

Crab pulsar and assume that the released energy is fully deposited at the bottom of the ejecta (“full deposition”) or deposited pursuant to the same one-group transport as γ -rays from the radioactive decay (“one-group transport”).

3. EVOLUTION OF ELECTRON-CAPTURE SUPERNOVAE

In the explosion of the model with $M_{\text{env}} = 3.0M_{\odot}$ and $X_{\text{env}}(\text{H}) = 0.2$ (Figs. 3a-3b), a shock wave is accelerated up to $9.6 \times 10^4 \text{ km s}^{-1}$ during the first 0.1 s due to the steep density gradient at the bottom of the envelope and decelerated down to $1.4 \times 10^3 \text{ km s}^{-1}$ by shock emergence from the stellar surface. Such drastic deceleration of shock develops severe Rayleigh-Taylor instability.

At the shock emergence, the ECSN flashes (Fig. 4a). The phenomenon is called a shock breakout, bolometrically brightest. Hereafter, we set $t = 0$ at the shock breakout. A peak wavelength at the shock breakout is $\sim 200 \text{ \AA}$ and bolometric luminosity is as bright as $L = 2.4 \times 10^{44} \text{ erg s}^{-1}$. Adopting a dust evaporation radius (Dwek 1983) and evaporation temperature for a short flash (Pearce & Mayes 1986), the shock breakout can destroy circumstellar dust up to $\sim 9.6 \times 10^{11} \text{ km}$ for a case of carbon dust.

As the SN ejecta cools down, the ECSN enters a plateau phase lasting $t_{\text{plateau}} \sim 60 - 100$ days. Plateau luminosity is $L_{\text{plateau}} \sim 10^{42} \text{ erg s}^{-1}$, which is as bright as typical Type II plateau supernovae (SNe II-P, e.g., SN 2004et, Sahu et al. 2006), and a photospheric velocity at the plateau is $3000 - 4000 \text{ km s}^{-1}$, which is slightly slower than typical SNe II-P. The plateau luminosity is fainter and the duration is longer for an explo-

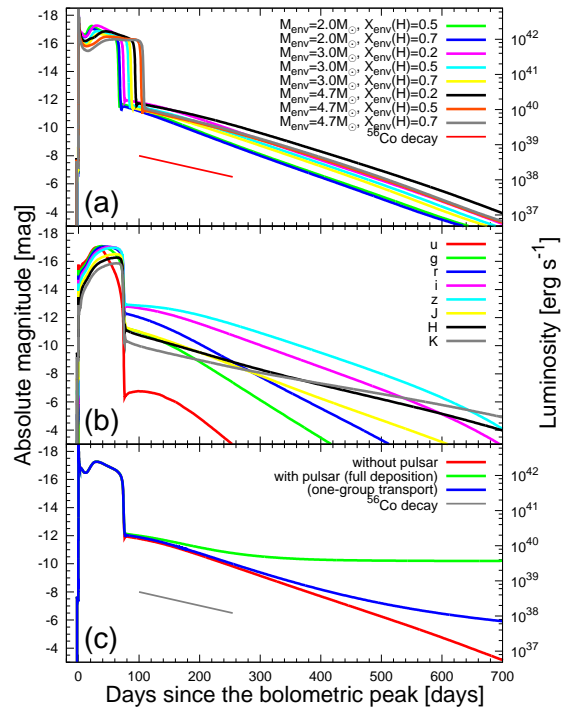


FIG. 4.— (a) Bolometric light curves of the ECSNe. The colors are the same as Figure 1 but the red line shows the energy release rate of ^{56}Co radioactive decay. (b) Multicolor light curves (red: u , green: g , blue: r , magenta: i , cyan: z , yellow: J , black: H , and gray: K) of the ECSN of the SAGB star with $M_{\text{env}} = 3.0M_{\odot}$ and $X_{\text{env}}(\text{H}) = 0.2$. (c) Bolometric light curves of the ECSNe without the pulsar contribution (red), with the full deposition (green), and with the one-group transport (blue). The energy release rate of ^{56}Co radioactive decay (gray) is also shown.

sion of a star with larger M_{env} and higher $X_{\text{env}}(\text{H})$. The plateau is followed by a tail. The luminosity suddenly fades by ~ 4 mag at the transition because of the small $M(^{56}\text{Ni})$. The tail luminosity declines gradually at a rate of $0.012 - 0.016 \text{ mag/day}$ that is slightly faster than an energy release rate from the ^{56}Co decay.

Multicolor light curves of the model with $M_{\text{env}} = 3.0M_{\odot}$ and $X_{\text{env}}(\text{H}) = 0.2$ are shown in Figure 4b. Photospheric temperature decreases after the shock breakout. Thus, the peak wavelength shifts to redder bands with time and optical luminosity increases gradually. Light curves in bluer bands peak at earlier epochs, e.g., $t \sim 10$ days in u band and $t \sim 20$ days in g band. In contrast to typical SNe II-P, the u and g light curves do not show a plateau and begin to decline immediately after the peak. Light curves in redder bands than i band peak at the end of the plateau. The multicolor light curves drop at the transition to the tail as the bolometric light curve does. Decline rates of the tail are higher for bluer bands.

Pulsar spin-down influences only the tail because the spin-down luminosity of the Crab pulsar is much fainter than the plateau luminosity. The ECSN shines with the energy release from ^{56}Co decay at the beginning of the tail and then the energy release from the newborn pulsar becomes dominant at a late phase ($t \gtrsim 250$ days, Fig. 4c). The tail luminosity is floored in the full deposition model, while the decline rate is lowered in the one-group transport model. The tail luminosity can be $\sim 2 - 6$ mag brighter than the model without the pulsar

contribution at $t = 600$ days.

4. COMPARISON WITH THE OBSERVATIONS

4.1. Crab Nebula and SN 1054

The Crab Nebula is the most famous and conspicuous supernova remnant. Optical and UV observations illustrate that the Crab Nebula is notably He-rich [$X(\text{He}) \sim 0.6 - 0.9$, e.g., MacAlpine & Satterfield 2008]. In addition to the He-rich abundance, a small ejecta mass ($M_{\text{ej}} = 4.6 \pm 1.8 M_{\odot}$, Fesen et al. 1997) and low kinetic energy ($E < 3 \times 10^{49}$ erg,⁷ e.g., Frail et al. 1995) suggest that the Crab Nebula is a remnant of the ECSN.

An expansion of the Crab Nebula was discovered in the early 1920s (Duncan 1921) and, in the same year, proximity of the Crab Nebula to SN 1054 was indicated (Lundmark 1921). An explosion date estimated by turning back the expansion is consistent with SN 1054 (Rudie et al. 2008). Hence, it is widely believed that the expanding Crab Nebula is a remnant of SN 1054.

A sudden appearance of SN 1054 had been recorded by medieval people and its optical light curve is enscrolled in historiographies (Pskovskii 1985; Stephenson & Green 2002). They described dates of first and last sightings and brightness. However, the medieval observations were rough and unconfident. Thus, reliability of the archives is deeply scrutinized by Stephenson & Green (2002). Referring to its conclusion, we adopt following three points with errorbars of 1 mag and 20 days; (1) SN 1054 was as bright as Venus (optical magnitude $m_{\text{opt}} \sim -3.5 - -5$) on 4 Jul 1054 and might be visible earlier than 4 Jul 1054 (e.g., 10 May 1054), (2) SN 1054 was visible in daytime for 23 days from 4 Jul 1054 and $m_{\text{opt}} \sim -3$ on 27 Jul 1054, and (3) SN 1054 disappeared in night on 6 Apr 1056 with $m_{\text{opt}} \sim 6$. We correct distance ($D = 2$ kpc, Trimble 1973) and reddening [$E(B - V) = 0.52$, Miller 1973] to the Crab Nebula.

We compare an “optical”⁸ light curve of the model with $M_{\text{env}} = 3.0 M_{\odot}$ and $X_{\text{env}}(\text{H}) = 0.2$ against the observations of SN 1054 (Fig. 5a). Here, an optical peak of the model is set to be 4 Jul 1054. The ECSN model well reproduces the bright and short plateau of SN 1054. The epoch of the transition from the plateau to the tail corresponds to the date at which SN 1054 had disappeared from the daytime sky.

The tail luminosities of the full deposition and one-group transport models are brighter and fainter than SN 1054, respectively. If the deposition efficiency is the middle of these models, a gradually-declining optical light curve can cross with the last observation of SN 1054. We note that the last point of SN 1054 is not compatible with the ECSN model without the pulsar contribution as suggested in Sollerman et al. (2001).

4.2. SN 2008S

SN 2008S is suggested to be its ECSN because the progenitor is bright and surrounded by dust and because SN 2008S is faint and evolves slowly (Botticella et al. 2009). However, the plateau luminosity of ECSN is

⁷ Here, $M_{\text{ej}} = 1 - 2 M_{\odot}$ is assumed. The kinetic energy is doubled by adopting $M_{\text{ej}} = 4.6 \pm 1.8 M_{\odot}$.

⁸ An optical band-pass is assumed to be a normal distribution with a peak at 5550 Å and a root-mean-square deviation of 550 Å (Vos 1978).

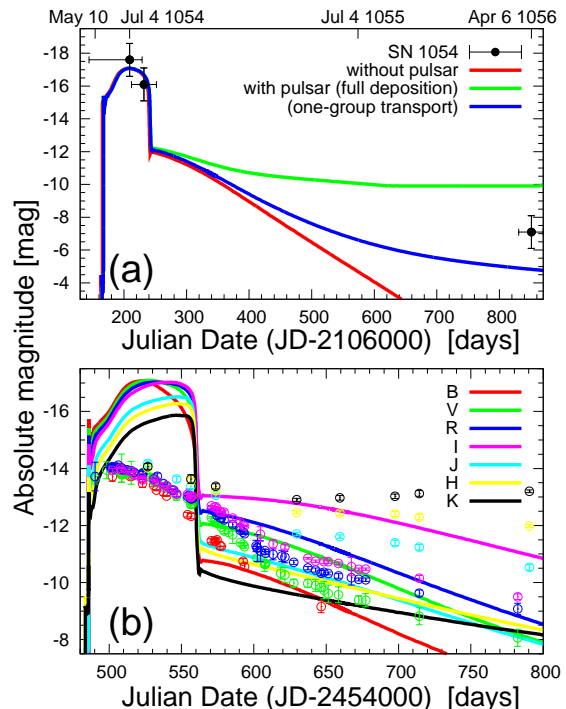


FIG. 5.— (a) Optical light curves of SN 1054 (black circles) and the ECSNe of the SAGB stars. The colors are the same as Fig. 4c. (b) Multicolor light curves of SN 2008S (red: B , green: V , blue: R , magenta: I , cyan: J , yellow: H , and black: K) are compared with those of the ECSN of the SAGB star with $M_{\text{env}} = 3.0 M_{\odot}$ and $X_{\text{env}}(\text{H}) = 0.2$.

as bright as that of normal SNe II-P due to the large presupernova radius (Fig. 4a). Thus, we conclude that the ECSN model based on the first-principle simulation (Kitaura et al. 2006) is incompatible with the faintness of SN 2008S (Fig. 5b).

However, there is a caveat that the plateau luminosity and duration depend on E and M_{env} ($L_{\text{plateau}} \propto E^{5/6} M_{\text{env}}^{-1/2}$ and $t_{\text{plateau}} \propto E^{-1/6} M_{\text{env}}^{1/2}$, Litvinova & Nadezhin 1985; Popov 1993; Eastman et al. 1994). If an explosion energy may be different for individual ECSNe, e.g., due to rotation, the faint and slowly-evolving SN 2008S could be explained. Applying the scaling laws and taking $L_{\text{plateau}} \sim 1 \times 10^{41}$ erg s^{-1} and $t_{\text{plateau}} \sim 140$ days of SN 2008S, we can derive its explosion properties; $E \sim 3.5 \times 10^{48}$ erg and $M_{\text{env}} \sim 3.4 M_{\odot}$. A series of first-principle simulation and light curve calculations are required to confirm that such the explosion is feasible and explains the multicolor light curves of SN 2008S.

5. DISCUSSION AND CONCLUSION

We present multicolor light curves of ECSNe with various M_{env} and $X_{\text{env}}(\text{H})$ based on the results of the first-principle simulation (Kitaura et al. 2006). We demonstrate that the shock breakout has peak luminosity of $L \sim 2 \times 10^{44}$ erg s^{-1} and can evaporate circumstellar dust up to $R \sim 10^{12}$ km for the case of carbon dust and that the plateau luminosity and duration of ECSNe are $L_{\text{plateau}} \sim 10^{42}$ erg s^{-1} and $t_{\text{plateau}} \sim 60 - 100$ days, respectively. The brighter and shorter plateau is realized by the model with smaller M_{env} and lower $X_{\text{env}}(\text{H})$. The plateau is followed by the tail with the luminosity drop

by ~ 4 mag.

The tail luminosity declines by $0.012 - 0.016$ mag/day for the model without the pulsar contribution, while, if the pulsar contributes to the light curve, the tail light curve is floored or the decline rate is lowered. The contribution from the pulsar spin-down luminosity as bright as the Crab pulsar is prominent only in the tail.

Furthermore, we compare the theoretical models with the ECSN candidates: SN 1054 and SN 2008S.

The bright and short plateau and low explosion energy of the ECSN model are consistent with SN 1054. The plateau is not reproduced with a low-energy explosion of a red supergiant star with heavy M_{env} . The tail luminosity of SN 1054 could be explained by the spin-down luminosity of the newborn Crab pulsar. Therefore, SN 1054 is likely to be the ECSN. The deceleration of the shock wave in ECSN (Figs. 3a-3b) is also favorable to produce filamentary structures observed in the Crab Nebula (e.g., Fesen et al. 1997).⁹

The optical light curve of SN 1054 constrains the initial spin-down luminosity of the Crab pulsar. Radio observations suggest $\tau_{\text{sd}} \leq 30$ yr and $L_{\text{sd},0} \sim 1.5 \times 10^{42}$ erg s⁻¹ to produce relic relativistic electrons (Atoyan 1999). However, such high $L_{\text{sd},0}$ leads to much brighter optical luminosity than SN 1054 at 6 Apr 1056. Our result favors $\tau_{\text{sd}} \sim 700$ yr and $L_{\text{sd},0} \sim 3.3 \times 10^{39}$ erg s⁻¹. These are also supported by a broad spectral evolution model of the pulsar wind nebula (Tanaka & Takahara 2010).

The typical ejecta velocity of the ECSN model with $M_{\text{env}} = 3.0M_{\odot}$ and $X_{\text{env}}(\text{H}) = 0.2$ is $v \sim 2.2 \times 10^3$ km s⁻¹, which is consistent with the low expansion velocity of the Crab Nebula (Rudie et al. 2008). On the other hand, the velocity of a wind blown from the progenitor is 29 km s⁻¹. Adopting the duration of the SAGB phase ($\sim 10^4$ yr, Nomoto et al. 1982; Siess 2007), the SAGB wind extends only upto 9.1×10^{12} km ($= 0.30$ pc), which is similar to an apparent size of the Crab Nebula (e.g., Rudie et al. 2008). The radius is smaller than the typical ejecta location of 6.9×10^{13} km ($= 2.2$ pc). Therefore, the forward shock should locate in a low-density circumstellar wind blown at the core He-burning phase or in an interstellar medium. This can be a reason why the forward shock of the Crab Nebula has not been found.

On the other hand, the plateau of the ECSN model is much brighter than that of SN 2008S. If the explosion energy of ECSNe is exactly 1.5×10^{50} erg as derived by the first-principle simulation (Kitaura et al. 2006), the multicolor light curves of the ECSN are inconsistent with those of SN 2008S. However, there could be a caveat that the explosion energy may vary on individual ECSNe. The ECSN explosion with $E \sim 3.5 \times 10^{48}$ erg and $M_{\text{env}} \sim 3.4M_{\odot}$ might be compatible with SN2008S.

⁹ The filamentary structures can also be originated by interaction between the ECSN ejecta and a pulsar wind nebula (Hester 2008 for a review). However, the structures exist even in the ejecta unaffected by the pulsar (e.g., Rudie et al. 2008). Future 3D calcu-

If SN 2008S is the ECSN with $E \sim 3.5 \times 10^{48}$ erg and $M_{\text{env}} \sim 3.4M_{\odot}$, we can speculate on shock breakout luminosity and $M(^{56}\text{Ni})$; According to analytic dependence (Matzner & McKee 1999), the luminosity of the shock breakout are $\sim 1.4 \times 10^{42}$ erg s⁻¹. Carbon dust at $\lesssim 9.2 \times 10^{10}$ km is evaporated by the shock breakout. The size of a dust-free cavity is roughly consistent with that estimated from a midinfrared observation of SN 2008S (Botticella et al. 2009). The explosion energy is comparable to a gravitational binding energy of the progenitor at $M \geq 1.3758M_{\odot}$. Thus, SN 2008S is likely to eject materials above the outer edge of the core and yield $M(^{56}\text{Ni}) \sim 4.4 \times 10^{-4}M_{\odot}$, which is slightly smaller than an estimate from the observed tail of SN 2008S (Botticella et al. 2009). Therefore, we propose that the light curve tail of SN 2008S is powered by a spin-down luminosity of a newborn neutron star as SN 1054. We note a caveat that SN 2008S is a Type II_n SN and thus could be contributed by interaction with circumstellar medium (e.g., Smith 2013).

The number of SNe sharing the characteristics of the ECSN, i.e., a bright and short plateau and faint tail, is small, if the SN 2008S-like transients are not the ECSNe. We also note that faint and low-energy SNe II-P, e.g., SN 1997D and SN 1999br (Zampieri et al. 2003), have a slower photospheric velocity at the plateau ($v \sim 1000 - 2000$ km s⁻¹) than the ECSN. The scarcity of the ECSNe might stem from a small mass range of a star ending up as ECSNe at solar metallicity (Langer 2012, for a review). Since significant contribution of ECSNe to the production of ⁴⁸Ca, ⁶⁴Zn, and ⁹⁰Zr is suggested (Wanajo et al. 2009, 2011, 2013), chemical evolution models taking into account the scarcity is required to study the origin of these isotopes.

We would like to thank Shuta J. Tanaka and Keiichi Maeda for fruitful discussion on Crab Pulsar and SNe II-P, respectively, and Shinya Wanajo for providing the abundance distribution. Data analysis were in part carried out on the general-purpose PC farm at Center for Computational Astrophysics, National Astronomical Observatory of Japan. This research has been supported in part by the RFBR-JSPS bilateral program, World Premier International Research Center Initiative, MEXT, Japan, and by the Grant-in-Aid for Scientific Research of the JSPS (23224004, 23540262, 23740157) and MEXT (23105705). S.B. is supported by the Grants of the Government of the Russian Federation 11.G34.31.0047, RF Sci. School 5440.2012.2 and 3205.2012.2 and by a grant IZ73Z0-128180/1 of the Swiss National Science Foundation (SCOPEs).

lations will test how the shock deceleration produces the filamentary structures.

REFERENCES

- Atoyan, A. M. 1999, *A&A*, 346, L49
 Blinnikov, S., Lundqvist, P., Bartunov, O., Nomoto, K., & Iwamoto, K. 2000, *ApJ*, 532, 1132
 Blinnikov, S. I., Eastman, R., Bartunov, O. S., Popolitov, V. A., & Woosley, S. E. 1998, *ApJ*, 496, 454
 Blinnikov, S. I., Röpke, F. K., Sorokina, E. I., Gieseler, M., Reinecke, M., Travaglio, C., Hillebrandt, W., & Stritzinger, M. 2006, *A&A*, 453, 229
 Bond, H. E., Bedin, L. R., Bonanos, A. Z., Humphreys, R. M., Monard, L. A. G. B., Prieto, J. L., & Walter, F. M. 2009, *ApJ*, 695, L154

- Botticella, M. T. et al. 2009, MNRAS, 398, 1041
- Bruenn, S. W. et al. 2013, ApJ, 767, L6
- Burrows, A. 2013, Reviews of Modern Physics, 85, 245
- Burrows, A., Dessart, L., & Livne, E. 2007, in American Institute of Physics Conference Series, Vol. 937, Supernova 1987A: 20 Years After: Supernovae and Gamma-Ray Bursters, ed. S. Immler, K. Weiler, & R. McCray, 370–380
- Duncan, J. C. 1921, Proceedings of the National Academy of Science, 7, 179
- Dwek, E. 1983, ApJ, 274, 175
- Eastman, R. G., Woosley, S. E., Weaver, T. A., & Pinto, P. A. 1994, ApJ, 430, 300
- Fesen, R. A., Shull, J. M., & Hurford, A. P. 1997, AJ, 113, 354
- Frail, D. A., Kassim, N. E., Cornwell, T. J., & Goss, W. M. 1995, ApJ, 454, L129+
- Hester, J. J. 2008, ARA&A, 46, 127
- Hoffman, R. D., Müller, B., & Janka, H. 2008, ApJ, 676, L127
- Janka, H., Müller, B., Kitaura, F. S., & Buras, R. 2008, A&A, 485, 199
- Janka, H.-T., Hanke, F., Huedepohl, L., Marek, A., Mueller, B., & Obergaulinger, M. 2012, ArXiv e-prints, 1211.1378
- Kitaura, F. S., Janka, H., & Hillebrandt, W. 2006, A&A, 450, 345
- Kotake, K., Sumiyoshi, K., Yamada, S., Takiwaki, T., Kuroda, T., Suwa, Y., & Nagakura, H. 2012, Progress of Theoretical and Experimental Physics, 2012, 301
- Langer, N. 2012, ARA&A, 50, 107
- Litvinova, I. Y., & Nadezhin, D. K. 1985, Soviet Astronomy Letters, 11, 145
- Lundmark, K. 1921, PASP, 33, 225
- MacAlpine, G. M., & Satterfield, T. J. 2008, AJ, 136, 2152
- Matzner, C. D., & McKee, C. F. 1999, ApJ, 510, 379
- Miller, J. S. 1973, ApJ, 180, L83+
- Miyaji, S., & Nomoto, K. 1987, ApJ, 318, 307
- Miyaji, S., Nomoto, K., Yokoi, K., & Sugimoto, D. 1980, PASJ, 32, 303
- Nomoto, K. 1984, ApJ, 277, 791
- . 1987, ApJ, 322, 206
- Nomoto, K., Sugimoto, D., Sparks, W. M., Fesen, R. A., Gull, T. R., & Miyaji, S. 1982, Nature, 299, 803
- Pearce, G., & Mayes, A. J. 1986, A&A, 155, 291
- Popov, D. V. 1993, ApJ, 414, 712
- Prieto, J. L. et al. 2008, ApJ, 681, L9
- Pskovskii, I. P. 1985, *Novye i sverkhnovye zvezdy*, ed. Pskovskii, I. P.
- Rudie, G. C., Fesen, R. A., & Yamada, T. 2008, MNRAS, 384, 1200
- Sahu, D. K., Anupama, G. C., Srividya, S., & Muneer, S. 2006, MNRAS, 372, 1315
- Saio, H., Nomoto, K., & Kato, M. 1988, ApJ, 331, 388
- Siess, L. 2007, A&A, 476, 893
- Smith, N. 2013, ArXiv e-prints, 1304.0689
- Sollerman, J., Kozma, C., & Lundqvist, P. 2001, A&A, 366, 197
- Stephenson, F. R., & Green, D. A. 2002, *Historical supernovae and their remnants*, by F. Richard Stephenson and David A. Green. International series in astronomy and astrophysics, vol. 5. Oxford: Clarendon Press, 2002, ISBN 0198507666, 5
- Szczygiel, D. M., Kochanek, C. S., & Dai, X. 2012, ApJ, 760, 20
- Tanaka, S. J., & Takahara, F. 2010, ApJ, 715, 1248
- Trimble, V. 1973, PASP, 85, 579
- Vos, J. J. 1978, Color Research & Application, 3, 125
- Wanajo, S., Janka, H.-T., & Müller, B. 2011, ApJ, 726, L15
- . 2013, ApJ, 767, L26
- Wanajo, S., Nomoto, K., Janka, H., Kitaura, F. S., & Müller, B. 2009, ApJ, 695, 208
- Zampieri, L., Pastorello, A., Turatto, M., Cappellaro, E., Benetti, S., Altavilla, G., Mazzali, P., & Hamuy, M. 2003, MNRAS, 338, 711